



## 2D COMPUTATIONAL STUDY OF THE AERODYNAMICS OF THE S4110 AIRFOIL AT LOW WIND SPEEDS USING QBLADE AND XFLR5

Bui Van Hung<sup>1,\*</sup>, Vu Minh Phap<sup>2</sup>, Le Quang Sang<sup>2</sup>, Vu Duy Duc<sup>1</sup>, Nguyen Quang Hoa<sup>1</sup>

<sup>1</sup>University of Transport and Communications, No 3 Cau Giay Street, Hanoi, Vietnam

<sup>2</sup>Institute of Science and Technology for Energy and Environment, Vietnam Academy of Science and Technology, 18 Hoang Quoc Viet Street, Hanoi 100000, Vietnam

### ARTICLE INFO

TYPE: Research Article

Received: 23/02/2025

Revised: 08/04/2025

Accepted: 10/05/2025

Published online: 15/05/2025

<https://doi.org/10.47869/tcsj.76.4.2>

\* *Corresponding author*

\* Email: hungtkm@utc.edu.vn; Phone: +84988333926

**Abstract:** The design of the wind turbine blades has a significant impact on the operation of the wind turbine. Therefore, the cross-sectional structure of the airfoil needs to be simulated by specialized software to evaluate the impact on the performance of the wind turbine, especially in the low wind speed region. This paper studies the aerodynamic characteristics such as lift coefficient ( $C_L$ ), drag coefficient ( $C_D$ ) and ratio ( $C_L/C_D$ ) in the attack angle ranges from -8 degrees to 10 degrees of the S4110 airfoil model under low wind velocity (3 m/s) using QBLADE and XFLR5 software with Reynolds coefficient margin conditions of 200000, Mach coefficient of 0.3 and Ncrit coefficient of 9. Evaluate the ability to analyze aerodynamic parameters. The purpose of the study is to verify the accuracy of the two software in wind turbine design under low wind velocity by comparing the simulation results with experimental data from Airfoiltool. The results showed that both the QBLADE and XFLR5 achieve high accuracy at small attack angles (from -4.5 degrees to 4 degrees), with an error of less than 5%. Besides, the optimal angle of attack of the model is determined with the value of 4 degrees and a Ratio ( $C_L/C_D$ ) value of 80.02.

**Keywords:** lift coefficient, drag coefficient, Reynolds coefficient, airfoil, CFD method, XFLR5.

@ 2025 University of Transport and Communications

## 1. INTRODUCTION

Wind energy has become one of the most important renewable energy sources in the world [1]. The first wind turbine was built in Scotland [2] with the Savonius vertical shaft design to supply power. There were many researches on the design and performance optimization of wind turbine blades in the world. Mustafa Alaskari et al.[3] optimized the performance of horizontal axis wind turbine blades (HAWT) at low power levels using the blade momentum element (BEM) method and QBLADE software, the research focused on optimizing design parameters such as torsion angle and arc length of turbine blades. The results showed that the optimum value of the lift-to-drag ratio ( $C_L/C_D$ ) was achieved at an attack angle of 2 degrees, while the optimum performance of the rotor occurred when the airfoil tip speed ratio reached 8. In addition, the study demonstrated the usefulness and high accuracy of QBLADE software, especially in the design and simulation of wind turbines under different operating conditions. D. Zahariea's research team [4] estimated the aerodynamic analysis process and the structure of a small horizontal axis wind turbine with a power level of 10kW using QBLADE software. The results showed that this software not only supports well in wind turbine design and simulation but also provides accurate evaluations of the performance and safety of the blades. In particular, analyses indicated that losses at the tip and base of the blades have a significant effect on turbine performance, emphasizing the role of this factor in the design process. Fazlar Rahman et al. used XFLR5 and QBLADE to numerically analyze a modified NACA 4412 airfoil for the lift-to-drag ratio ( $C_L/C_D$ ) in Vertical Axis Wind Turbines (VAWTs) at a low Reynolds number ( $1.22 \times 10^5$ ) [5]. The study results showed that the highest power coefficient ( $C_p$ ) values are 0.387 (TSR = 2.4, SR = 0.33) and 0.365 (TSR = 2.6, SR = 0.17), exceeding the performance of the baseline NACA 4412 airfoil and complying with the Betz limit ( $C_p = 0.59$ ). The modified airfoil demonstrated potential for application in VAWTs on urban and suburban rooftops at low wind speeds. Yash Shah et al. improved the efficiency of Airborne Wind Energy Systems (AWES) by developing high-performance airfoils based on the CLark-Y airfoil [6] with the support of XFLR software. Various modifications in camber and thickness were tested to optimize the lift-to-drag ratio ( $C_L/C_D$ ). The best-performing designs led to the creation of a new airfoil series which demonstrated a 26.92% performance improvement. R. S. Jegan Vishnu and Beena D. Baloni explored the use of buoyant airfoil-shaped balloons to harness high-altitude wind energy in India, where 45 TWh of wind power has been utilized over a decade at lower altitudes [7]. Different NACA 4-digit airfoils were analyzed in the XFLR5 program by varying thickness, camber, and camber position to minimize drag. The study results showed that NACA 1730 has the lowest drag coefficient ( $8.345 \times 10^{-3}$  at 0 degrees).

In Vietnam, the natural conditions with a long coastline and monsoon climate offer great potential for wind energy development. However, the wind regime in urban areas is characterized by low and unstable wind speeds due to obstruction by tall buildings, which significantly affects the stability of conventional wind turbine operation. On the other hand, turbulence and wind vortices also reduce efficiency and cause faster wear on the wind turbines. Therefore, the challenge is to conduct research to design blade models suitable for the specific wind conditions in urban areas in Vietnam. Domestic research has focused on improving airfoil design to increase performance. Dinh Bao Anh et al proposed an efficient low-speed airfoil design and optimization process using multi-fidelity analysis for small unmanned aerial vehicles, in which XFLR5 is used as an analysis tool [8]. Le Quang Sang et al. used XFLR5 and CFD methods to increase the aerodynamic performance of the S1010 airfoil when operating at low wind speed [9]. Dinh Van Thin et al. selected XFLR5 software to improve the

NACA6409 airfoil and increase aerodynamic performance in low wind conditions from 3 m/s to 5 m/s [10]. The NACA64A010 airfoil model was simulated by the XFLR5 software and the Ansys software to determine the change in comparison with the experimental parameters [11]. The difference between the results of Ansys Fluent and XFLR5 is straightforward. Ansys Fluent detail establishes input parameters such as computational grids, boundary conditions and turbulence models, and uses complex numerical methods to simulate flow with high accuracy, especially in large Reynolds numbers. These factors help Ansys Fluent accurately reproduce nonlinear aerodynamic phenomena and turbulent flow effects. In contrast, XFLR5 uses approximation methods such as the thin plate method, which is limited in accurately simulating complex aerodynamic phenomena. However, the XFLR5 remains a useful tool in the early design phase, when it is necessary to quickly evaluate designs without requiring absolute high accuracy. These studies not only contribute to improving the performance of small wind turbines in Vietnam but also affirm the role of simulation tools in turbine blade design and optimization to provide more data information about the wind turbine blade design calculations.

In this study, the S4110 airfoil model is chosen for analysis because of its good performance in low wind conditions in urban areas. The QBLADE and XFLR5 software will be used to calculate aerodynamic coefficients such as lift ( $C_L$ ), drag ( $C_D$ ), and  $C_L/C_D$  ratio. The results from the two software will be compared with the empirical data on Airfoiltool to evaluate reliability. The study expects to provide useful information in the optimization of wind turbine blade design, especially for areas with weak wind conditions such as urban areas in Vietnam.

## 2. METHODOLOGY

### 2.1. Analysis Process

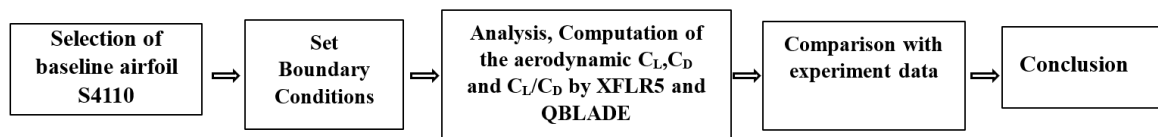


Figure 1. Diagram of the analysis process.

Figure 1 illustrates the procedure for analyzing the S4110 airfoil. The airfoil pattern is imported, setting the boundary conditions such as flow, tonnage angle, and environmental parameters. The data is then processed by XFLR5 and QBLADE to calculate the aerodynamic characteristics. The results from the two software were compared with experimental data to evaluate the accuracy and performance of the airfoil sample, as well as the reliability of the analysis method.

### 2.2. S4110 airfoil

The S4110 airfoil model is designed for horizontal axis wind turbines, it is selected in the Airfoiltool website [12] to provide an extensive database of airfoil sample configurations and support aerodynamic performance analysis. The website allows users to look up detailed information, and aerodynamic characteristics of hundreds of Airfoils models. In this paper, the S4110 airfoil is selected because it has a slim profile, optimized curvature, and thickness position to reduce drag while maintaining strong lifting capacity. As a result, this blade model is often used in small wind turbines with a capacity of less than 10 kW and equipment operating

in unstable wind conditions. The analysis results show that the S4110 can maintain good performance even at low Reynolds numbers, which is a common condition in small wind energy applications. The profile and parameters of the airfoil pattern are shown in Figure 2 and Table 1.

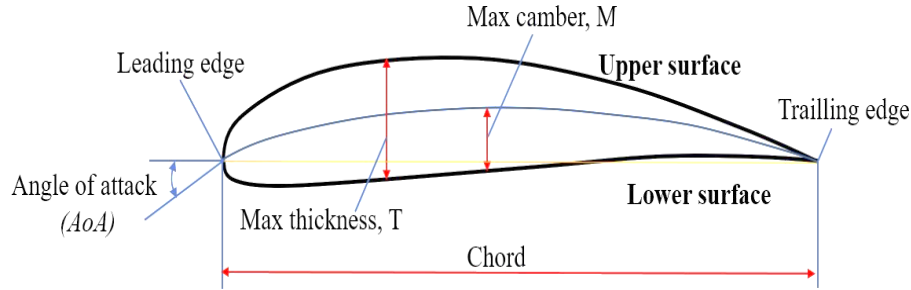


Figure 2. S4110 airfoil profile [12].

Table 1. S4110 airfoil specifications [12].

Specifications	Value
Straight line connecting the start and end point, Length	1 m
Maximum thickness	0.084 m at 26.6% of the length
Maximum Curvature	0.031 m at 45.4% of the length

### 2.3. Simulation software

This paper used two main software: QBLADE and XFLR5 for research. QBLADE uses Blade Element Momentum theory (BEM) to evaluate and analyze the aerodynamic parameters of the airfoil sample [13]. The XFLR5 uses the Bar Element Method or the control Panel Method (PM) algorithm [14]. Both software are recognized and used extensively by researchers in their studies, which contributes to improving the reliability of the aerodynamic statistics that both software analyzes. These aerodynamic parameters include  $C_L$ ,  $C_D$ , and related systems to calculate them as shown in the equations (1),(2),(3),(4) [15].

$$C_L = \frac{2L}{\rho \cdot v^2 \cdot A} \quad (1)$$

$$C_D = \frac{2D}{\rho \cdot v^2 \cdot A} \quad (2)$$

where:  $C_L$  and  $C_D$  are the lifting coefficient and the drag coefficient on the surface, respectively;  $L$  and  $D$  are lifting and dragging ( $\text{kg} \cdot \text{m}/\text{s}^2$ );  $A$  is the area of the airfoil pattern ( $\text{m}^2$ );  $\rho$  is the density of airflow ( $\text{kg}/\text{m}^3$ );  $v$  is the wind velocity ( $\text{m}/\text{s}$ ).

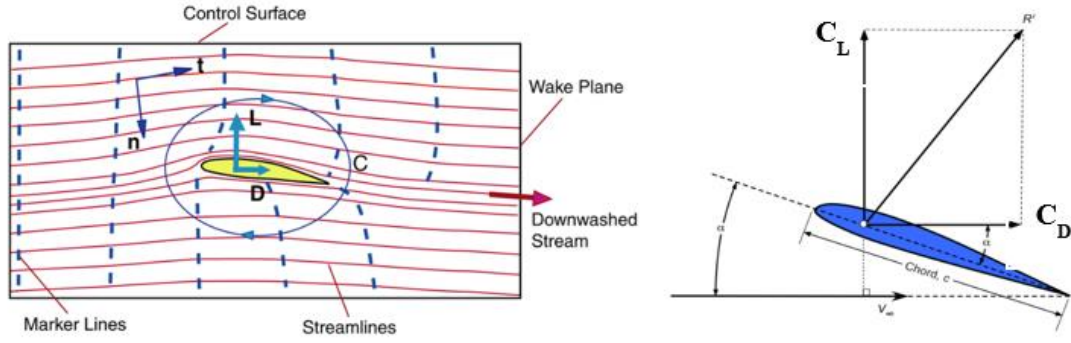


Figure 3. Impact of lifting and impeller coefficients on airfoil samples [16].

The Reynolds ( $Re$ ) number varies depending on the wind velocity to be studied [14]. In the study, the group used a  $Re$  of 200000, which corresponds to a low wind condition of 3 m/s.

$$Re = \frac{\rho \cdot v \cdot c}{\mu} \quad (3)$$

where:  $v$  is the wind velocity (m/s);  $\rho$  is the density of airflow ( $\text{kg/m}^3$ );  $\mu$  is the dynamic viscosity ( $\text{kg/m.s}$ );  $c$  is the length of the airfoil pattern (m).

The S4110 airfoil sample was analyzed at different angles of attack in the range of [-8 degrees to 10 degrees] under low wind velocity of 3 m/s, which is equivalent to Reynolds' number of 200000. The density of the airflow is  $1.225 \text{ kg/m}^3$  and the dynamic viscosity is  $1.789 \times 10^{-5} \text{ kg/m.s}$ . The static pressure distributed throughout space is 101325 Pa. Mach Coefficient ( $M$ ) is the ratio between the velocity of an object and the velocity of sound as can be seen in the formula (4) [17]. This study chose a Mach coefficient of 0.3 and a  $N_{crit}$  of 9 to ensure stability, focusing only on the analysis of the  $C_L$ ,  $C_D$ , and  $C_L/C_D$  ratios.

$$M = \frac{v}{a} \quad (4)$$

where:  $v$  is the velocity of the object (m/s);  $a$  is the velocity of sound in that environment (m/s).

#### a. QBLADE software

In this study, the QBLADE software use the coordinates of the S4110 airfoil model with the input parameters including a Reynolds coefficient of 200000, Mach coefficient of 0.3, and  $N_{crit}$  coefficient of 9 as shown in Figure 4.

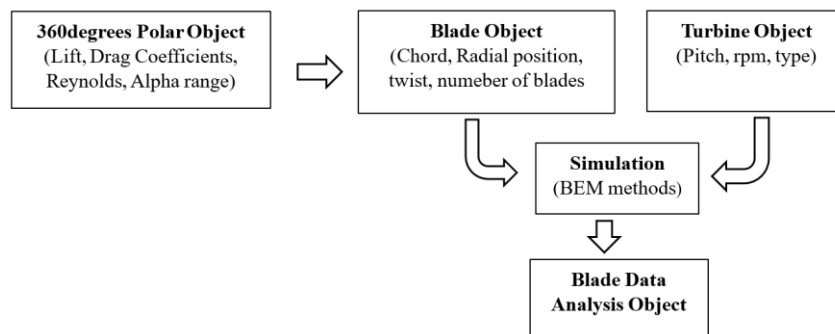


Figure 4. Analysis and design process in QBLADE software [3].

## b. XFLR5 Software

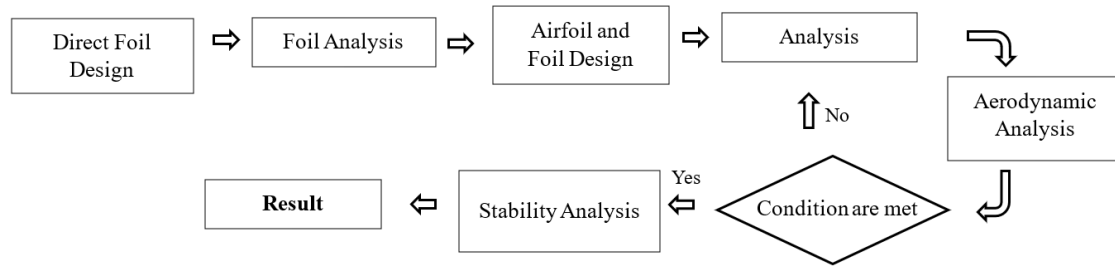


Figure 5. Analysis and design process in XFLR5 [18].

XFLR5 is an aerodynamic analysis software specialized for aircraft wings and airfoil models, utilizing both two-dimensional (2D) and three-dimensional (3D) computational methods. It employs the Panel Method combined with a Boundary Layer Model to calculate key aerodynamic parameters such as the lift coefficient ( $C_L$ ), drag coefficient ( $C_D$ ), and moment coefficient ( $C_M$ ). The input parameters include the Reynolds number ( $Re$ ), angle of attack ( $\alpha$ ), and flow conditions. This method allows for an accurate assessment of an airfoil's aerodynamic performance before applying it to actual designs. The analysis diagram of the software is shown in Figure 5. A comprehensive analysis of the aerodynamic characteristics of the S4110 airfoil was conducted using two computational tools, QBLADE and XFLR5. The resulting data provide clear insights into the airfoil's aerodynamic performance across a range of angles of attack.

We initially included Figures 6a and 6b in the previous version of the paper to present the simulation results from the two software programs, QBLADE and XFOIL. However, after careful consideration, we have decided to remove Figures 6a and 6b in the current version for the following reasons:

1. Space Constraints: Including both figures would significantly increase the total page count, making it exceed 15 pages, which could compromise the readability and overall presentation quality. Additionally, presenting these figures with sufficient resolution would not be feasible within the current layout.
2. Redundancy: The simulation results from both QBLADE and XFOIL are effectively demonstrated in Figures 6 and 7 in this revised version of the paper. We believe these figures sufficiently convey the key findings. For readers seeking further detailed analysis or clarification, we encourage them to reach out to the authors directly via email for further discussion.

## 3. RESULTS AND DISCUSSION

Table 2 and Table 3 present the analysis results of the aerodynamic parameters  $C_L$ ,  $C_D$ ,  $C_L/C_D$  and the percentage difference between these parameters and the experimental values with the help of QBLADE and XFLR5 software. The two tables above show the comparison of the aerodynamic parameters ( $C_L$ ,  $C_D$ ,  $C_L/C_D$ ) of the two software with the experimental values that have previously obtained on the Airfoiltools website. It can be seen that the data of the two software are almost the same and also close to the experimental values. However, at some angles, there is still a large difference.

Table 2. Comparison of aerodynamic parameters from QBLADE software with empirical values.

Angles of attack (AoA)	Lifting coefficient ( $C_L$ )			Drag coefficient ( $C_D$ )			$C_L/C_D$ Ratio		
	Expt	QBLADE	Error(%)	Expt	QBLADE	Error(%)	Expt	QBLADE	Error(%)
-8	-0.4121	-0.3425	-16.8891	0.0883	0.0923	4.5182	-4.6665	-3.7107	-20.4819
-7.5	-0.4160	-0.3421	-17.7644	0.0804	0.0870	8.2638	-5.1773	-3.9326	-24.0415
-7	-0.4184	-0.3520	-15.8700	0.0758	0.0825	8.7840	-5.5183	-4.2677	-22.6632
-6.5	-0.4272	-0.3802	-11.0019	0.0709	0.0795	12.2196	-6.0279	-4.7806	-20.6929
-6	-0.4298	-0.3960	-7.8641	0.0646	0.0766	18.5053	-6.6502	-5.1704	-22.2517
-4.5	-0.2428	-0.2420	-0.3295	0.0221	0.0329	49.1395	-10.9964	-7.3489	-33.1696
-4	-0.1739	-0.1716	-1.3226	0.0180	0.0223	24.1226	-9.6880	-7.7020	-20.5000
-3.5	-0.1005	-0.0904	-10.0498	0.0160	0.0173	7.7979	-6.2695	-5.2315	-16.5566
-3	-0.0254	-0.0102	-59.8425	0.0150	0.0149	-0.6008	-1.6956	-0.6850	-59.5998
-2.5	0.0449	0.0606	34.9666	0.0141	0.0148	5.0283	3.1799	4.0863	28.5049
-2	0.1190	0.1502	26.2185	0.0130	0.0134	3.5494	9.1821	11.1923	21.8921
-1.5	0.1941	0.2115	8.9645	0.0112	0.0120	7.0536	17.3304	17.6397	1.7850
-1	0.2537	0.2775	9.3812	0.0101	0.0106	4.5500	25.0940	26.2535	4.6210
-0.5	0.3372	0.3489	3.4698	0.0098	0.0100	2.1472	34.4785	34.9249	1.2947
0	0.4021	0.4186	4.1035	0.0096	0.0098	2.0921	42.0607	42.8893	1.9702
0.5	0.4617	0.4746	2.7940	0.0094	0.0098	3.7194	49.0648	48.6270	-0.8922
1	0.5157	0.5347	3.6843	0.0094	0.0097	3.6364	55.1551	55.1806	0.0463
1.5	0.5691	0.5932	4.2348	0.0093	0.0096	3.1049	60.9315	61.5992	1.0958
2	0.6221	0.6481	4.1794	0.0094	0.0097	3.3120	66.4637	67.0217	0.8396
2.5	0.6747	0.7039	4.3278	0.0094	0.0098	3.3934	71.5483	72.1949	0.9038
3	0.7259	0.7589	4.5461	0.0096	0.0099	3.6573	75.8516	76.5020	0.8575
3.5	0.7766	0.8121	4.5712	0.0098	0.0103	4.5918	79.2449	79.2293	-0.0197
4	0.8256	0.8634	4.5785	0.0102	0.0108	5.9921	81.1002	80.0185	-1.3337
4.5	0.8724	0.9099	4.2985	0.0108	0.0117	8.6351	81.0028	77.7692	-3.9919
5	0.9163	0.9542	4.1362	0.0117	0.0129	10.8155	78.6524	73.9117	-6.0274
5.5	0.9578	0.9968	4.0718	0.0128	0.0144	12.4025	74.7114	69.1742	-7.4115
6	0.9986	1.0422	4.3661	0.0142	0.0158	11.4165	70.3735	65.9203	-6.3279
6.5	1.0400	1.0865	4.4712	0.0156	0.0174	11.2179	66.6667	62.6225	-6.0663
7	1.0818	1.1305	4.5018	0.0170	0.0190	11.5746	63.5605	59.5313	-6.3391
7.5	1.1231	1.1711	4.2739	0.0185	0.0211	14.2857	60.7738	55.4498	-8.7604
8	1.1632	1.2075	3.8085	0.0200	0.0236	17.7645	58.0439	51.1653	-11.8508
8.5	1.2006	1.2448	3.6815	0.0219	0.0254	16.0201	54.7969	48.9693	-10.6349
9	1.2373	1.2748	3.0308	0.0238	0.0293	23.1384	52.0530	43.5531	-16.3293
9.5	1.2715	1.2974	2.0370	0.0258	0.0324	25.2420	49.2257	40.1051	-18.5281
10	1.3027	1.2959	-0.5220	0.0282	0.0385	36.4281	46.1623	33.6597	-27.0839

Table 3. Comparison of aerodynamic parameters from XFLR5 software with experimental values.

Angles of attack (AoA)	Lifting coefficient ( $C_L$ )			Drag coefficient ( $C_D$ )			$C_L/C_D$ Ratio		
	Expt	XFLR5	Error(%)	Expt	XFLR5	Error(%)	Expt	XFLR5	Error(%)
-8	-0.4121	-0.3425	-16.8891	0.0883	0.0923	4.5182	-4.6665	-3.7107	-20.4819
-7.5	-0.4160	-0.3421	-17.7644	0.0804	0.0870	8.2638	-5.1773	-3.9326	-24.0415
-7	-0.4184	-0.3520	-15.8700	0.0758	0.0825	8.7840	-5.5183	-4.2677	-22.6632
-6.5	-0.4272	-0.3802	-11.0019	0.0709	0.0795	12.2196	-6.0279	-4.7806	-20.6929
-6	-0.4298	-0.3960	-7.8641	0.0646	0.0766	18.5053	-6.6502	-5.1704	-22.2517
-4.5	-0.2428	-0.2420	-0.3295	0.0221	0.0329	49.1395	-10.9964	-7.3489	-33.1696
-4	-0.1739	-0.1716	-1.3226	0.0180	0.0223	24.1226	-9.6880	-7.7020	-20.5000
-3.5	-0.1005	-0.0904	-10.0498	0.0160	0.0173	7.7979	-6.2695	-5.2315	-16.5566
-3	-0.0254	-0.0102	-59.8425	0.0150	0.0149	-0.6008	-1.6956	-0.6850	-59.5998
-2.5	0.0449	0.0606	34.9666	0.0141	0.0148	5.0283	3.1799	4.0863	28.5049
-2	0.1190	0.1502	26.2185	0.0130	0.0134	3.5494	9.1821	11.1923	21.8921
-1.5	0.1941	0.2115	8.9645	0.0112	0.0120	7.0536	17.3304	17.6397	1.7850
-1	0.2537	0.2775	9.3812	0.0101	0.0106	4.5500	25.0940	26.2535	4.6210
-0.5	0.3372	0.3489	3.4698	0.0098	0.0100	2.1472	34.4785	34.9249	1.2947
0	0.4021	0.4186	4.1035	0.0096	0.0098	2.0921	42.0607	42.8893	1.9702
0.5	0.4617	0.4746	2.7940	0.0094	0.0098	3.7194	49.0648	48.6270	-0.8922
1	0.5157	0.5347	3.6843	0.0094	0.0097	3.6364	55.1551	55.1806	0.0463
1.5	0.5691	0.5932	4.2348	0.0093	0.0096	3.1049	60.9315	61.5992	1.0958
2	0.6221	0.6481	4.1794	0.0094	0.0097	3.3120	66.4637	67.0217	0.8396
2.5	0.6747	0.7039	4.3278	0.0094	0.0098	3.3934	71.5483	72.1949	0.9038
3	0.7259	0.7589	4.5461	0.0096	0.0099	3.6573	75.8516	76.5020	0.8575
3.5	0.7766	0.8121	4.5712	0.0098	0.0103	4.5918	79.2449	79.2293	-0.0197
4	0.8256	0.8634	4.5785	0.0102	0.0108	5.9921	81.1002	80.0185	-1.3337
4.5	0.8724	0.9099	4.2985	0.0108	0.0117	8.6351	81.0028	77.7692	-3.9919
5	0.9163	0.9542	4.1362	0.0117	0.0129	10.8155	78.6524	73.9117	-6.0274
5.5	0.9578	0.9968	4.0718	0.0128	0.0144	12.4025	74.7114	69.1742	-7.4115
6	0.9986	1.0422	4.3661	0.0142	0.0158	11.4165	70.3735	65.9203	-6.3279
6.5	1.0400	1.0865	4.4712	0.0156	0.0174	11.2179	66.6667	62.6225	-6.0663
7	1.0818	1.1305	4.5018	0.0170	0.0190	11.5746	63.5605	59.5313	-6.3391
7.5	1.1231	1.1711	4.2739	0.0185	0.0211	14.2857	60.7738	55.4498	-8.7604
8	1.1632	1.2075	3.8085	0.0200	0.0236	17.7645	58.0439	51.1653	-11.8508
8.5	1.2006	1.2448	3.6815	0.0219	0.0254	16.0201	54.7969	48.9693	-10.6349
9	1.2373	1.2748	3.0308	0.0238	0.0293	23.1384	52.0530	43.5531	-16.3293
9.5	1.2715	1.2974	2.0370	0.0258	0.0324	25.2420	49.2257	40.1051	-18.5281
10	1.3027	1.2959	-0.5220	0.0282	0.0385	36.4281	46.1623	33.6597	-27.0839

Figure 6 shows the dependence of the lift coefficient ( $C_L$ ) on the angle of attack (AoA) of the S4110 airfoil model, with data from experiments (Expt.) and QBLADE and XFLR5 simulations. In the negative angle of attack (-8 degrees to -6 degrees) region,  $C_L$  of the



experiment has a slight decrease in the negative angle of attack and gradually increases from -6 degrees to 10 degrees, but the empirical data are lower due to the influence of the entry boundary conditions, while QBLADE and XFLR5 both give the same results.

In the small angle of attack region (0 degrees to 5 degrees), all three methods are consistent and have high accuracy in the analysis of the calculation of the value of  $C_L$ . From 5 degrees to 10 degrees, the  $C_L$  gradually increases as it nears its maximum value, with a small deviation between the experiment and the simulation, mainly due to the actual margin conditions entered into the two software. It can be seen that computational analysis methods (QBLADE and XFLR5) work well in predicting trends across most regions. Small deviations in the negative attack angle region can be caused by practical factors such as boundary conditions, and simulation accuracy.

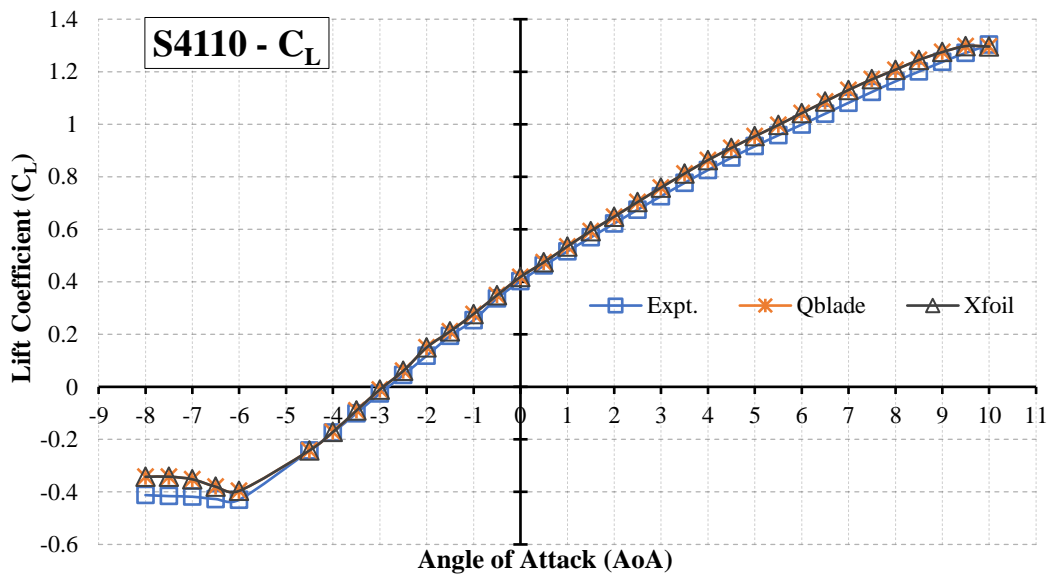


Figure 6. Lift coefficient ( $C_L$ ) versus Angle of Attack.

Figure 7 shows the drag coefficient ( $C_D$ ) in angle of attack (AoA) of the S4110 airfoil model, comparing the experimental data (Expt.) and simulations from QBLADE and XFLR5. In the small angle of attack region (-8 degrees to -4 degrees),  $C_D$  decreases rapidly and the similarity between the methods is quite high, although the experiment predicts a slightly higher value due to the influence of boundary conditions.  $C_D$  remains at its lowest value between -4 degrees and 5 degrees of angles of attack with three almost complete articulation methods. As the angle of attack increases (5 degrees to 11 degrees), the  $C_D$  gradually increases, reflecting greater aerodynamic drag, the error in this area can exceed the threshold of 30%, with some cases up to more than 36%. This is mainly due to the limitations of simulation tools such as QBLADE and XFLR5 in handling complex phenomena at high angles of attack. When the angle of attack is large (5 degrees to 10 degrees), the flow on the airfoil surface is prone to flow separation, creating a turbulent wake area behind the airfoil, and increasing aerodynamic drag. In addition, the separation flow does not only occur at a fixed location but spreads in a three-dimensional direction, especially at the airfoil edge, causing stronger tip vortices due to the large pressure difference between the top and bottom of the airfoil.

These phenomena increase the induction drag, but two-dimensional simulations are not capable of accurately simulating this three-dimensional effect. In addition, QBLADE and

XFLR5 are based on flow idealization assumptions (stable, non-turbulent), which leads to an underestimation of the complexity of the actual flow. In contrast, empirical data more accurately reflect these factors thanks to measurements in a real flow environment. Simulations from XFLR5 and QBLADE predict higher than experimental  $C_D$  at large angles of attack, mainly due to the ideal assumption in aerodynamic analysis models. Overall, the two analytical methods exhibit good compatibility, with small deviations concentrated in the negative and high angle of attack regions.

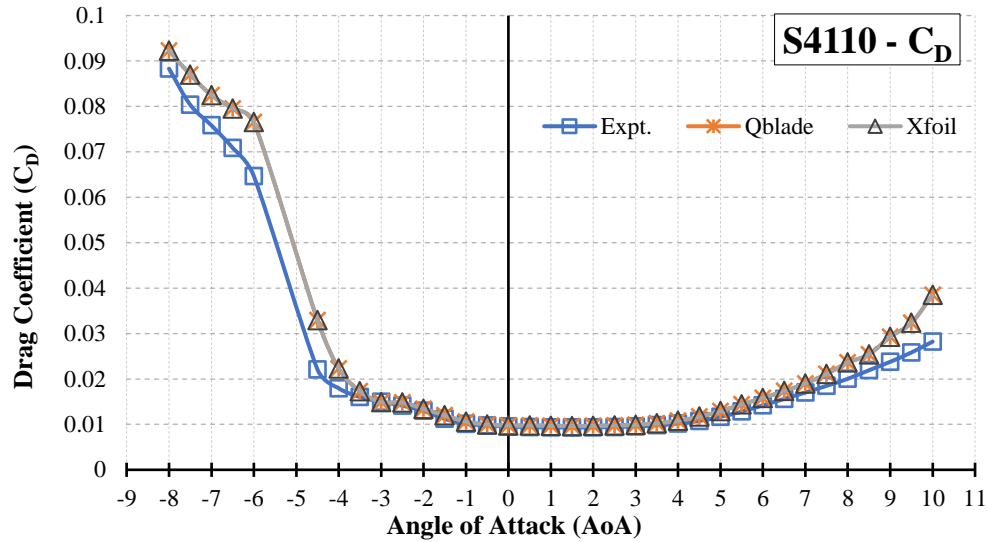


Figure 7. Drag coefficient ( $C_D$ ) versus Angle of Attack.

Figure 8 shows the ratio of lift coefficient to drag coefficient ( $C_L/C_D$ ). From -2.5 degrees to 2 degrees, the value of the simulated  $C_L/C_D$  was higher than the experimental one (deviation from 21.89% to 28.50%), reflecting the sensitivity of the theoretical models to the boundary layer in the transition region, leading to an underestimation of drag under real conditions. At the mean angle of attack (2.5 degrees to 4 degrees), the ratio between the data becomes quite consistent, with a deviation of less than 2%. However, at higher angles of attack (above 5 degrees), deviations begin to increase significantly, up to 17.08% at 10 degrees. This shows the inadequacy of the idealized models in predicting current separation and rapidly increasing drag at large angles of attack. It can be seen that the deviation between experiment and simulation comes from the limitations of XFLR5 and QBLADE in simulating actual flow, especially at extreme attack angles, where flow separation, turbulence, and three-dimensional influence become dominant. The data also underscore the strong reliance of simulation results on input assumptions, such as viscosity and flow conditions, which are difficult to accurately reproduce in practice.

The turbulence model undoubtedly has a significant impact on the numerical simulation results of wind turbine blades. The traditional numerical simulation process does not account for the effect of varying angles of attack on the simulation results. Regardless of the angle of attack, only a single turbulence model is applied to simulate the aerodynamic performance of the wind turbine blade. Therefore, these aerodynamic performance simulation methods tend to result in larger errors compared to advanced simulation tools, such as ANSYS Fluent. Computational fluid dynamics (CFD) is a branch of multi-physics system analysis that simulates fluid flow behavior and its thermodynamic properties using numerical models.

Advanced methods have the advantage of being able to address fluid dynamics issues, producing results that are closer to real-world conditions, improving and enhancing product efficiency without relying on costly and time-consuming physical experiments. Over the past decade, tools and methods have been continuously refined to increase productivity and reduce the time needed to achieve results.

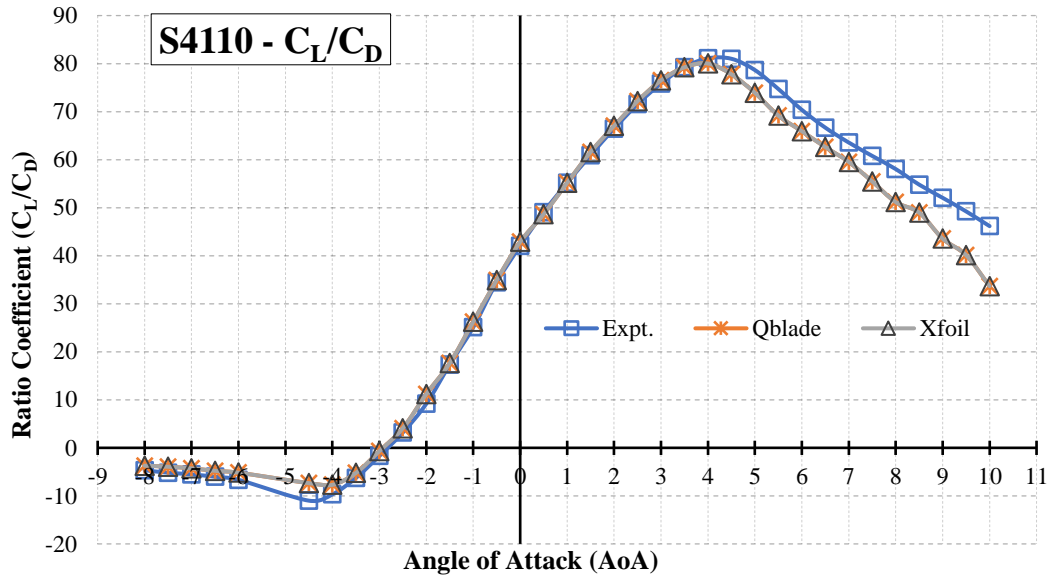


Figure 8.  $C_L/C_D$  Ratio versus Angle of Attack.

#### 4. CONCLUSION

The study used QBLADE and XFLR5 software to analyze the aerodynamics of the S4110 airfoil model under low wind conditions (3 m/s) with Re boundary conditions of 200000, Mach coefficient of 0.3, and Ncrit coefficient of 9. All three main factors including lift coefficient ( $C_L$ ), drag coefficient ( $C_D$ ), and lift/drag ratio ( $C_L/C_D$ ) show significant similarities between simulated and experimental values. The analysis shows that the lift coefficient gradually increases to a 10 degrees angle, however, the lift/drag ratio remains stable with a value of 80.02 at a 4 degrees angle of attack, which is equivalent to the experimental data. In particular, the two software allow the prediction of important aerodynamic parameters such as a maximum lift factor of 1.274 at a 9.5 degrees angle of attack, and an optimal lift/drag ratio of 80.02 at a 4 degrees angle. After the analysis, we have drawn out some of the advantages and disadvantages of the two software. Both software show high accuracy in predicting basic aerodynamic properties, with significant similarities to experimental data from Airfoiltool in the small angle of attack range. However, at high angles of attack and complex flows, the deviation between simulation and experiment increases significantly, reflecting the limitation in the ability to simulate complex aerodynamic phenomena. This poses a need to improve simulation tools and methods to improve accuracy. The study confirms the potential application of QBLADE and XFLR5 in aerodynamic analysis. Furthermore, the results of this study could influence the design of wind turbines and operational strategies in low-wind environments. Additionally, the study recommends the use of more advanced tools, such as ANSYS Fluent, for simulating more complex conditions. The research team will also focus on optimizing the design of wind turbine blades and enhancing performance predictions in variable wind environments, particularly in urban areas with low wind speeds.

## ACKNOWLEDGMENT

This research is funded by University of Transport and Communications (UTC) under grant number T2024-CK-008TD.

## REFERENCE

- [1]. J. F. Manwell, J. G. McGowan, A. L. Rogers, Wind Energy Explained: Theory, Design and Application, (2010). <https://doi.org/10.1002/9781119994367>
- [2]. B. Backwell, Wind power: The struggle for control of a new global industry: 2nd Edition, (2017). <https://doi: 10.4324/9781315112534>
- [3]. M. Alaskari, O. Abdullah, M. H. Majeed, Analysis of Wind Turbine Using QBlade Software, in IOP Conference Series: Materials Science and Engineering, (2019). <https://doi:10.1088/1757-899X/518/3/032020>
- [4]. D. Zahariea, D. E. Husaru, C. M. Husaru, Aerodynamic and structural analysis of a small-scale horizontal axis wind turbine using QBlade, in IOP Conference Series: Materials Science and Engineering, (2019).
- [5]. F. Rahman, S. W. Ul Huda, S. T. Sneha, J. Hossain, and M. Haque, Numerical Analysis of Modified NACA 4412 Airfoil for Implementation of Low Reynolds Numbers VAWTs, 51 (2022) 28–38.
- [6]. Yash Shah, Juhi Kothari, Mehek Shaikh, Ramesh Rajguru, Study of Performance Ratio of Newly Developed High-Performance Airfoil with Respect to the Airborne Wind Energy System, in Advances in Clean Energy and Sustainability, Springer Nature Singapore, 1 (2024) 347–356. [https://doi.org/10.1007/978-981-97-5415-1\\_29](https://doi.org/10.1007/978-981-97-5415-1_29)
- [7]. R. S. Jegan Vishnu, B. D. Baloni, Numerical Analysis of Buoyant Balloon for Airborne Wind Turbines, in Lecture Notes in Mechanical Engineering, (2023).
- [8]. B. A. Dinh, H. K. Ngo, and V. N. Nguyen, An efficient low-speed airfoil design optimization process using multi-fidelity analysis for UAV flying wing, Science and Technology Development Journal, 19 (2016) 43-52.
- [9]. Le Quang Sang, Tinnapob Phengpom, Dinh Van Thin, Nguyen Huu Duc, Le Thi Thuy Hang, Cu Thi Thanh Huyen, Nguyen Thi Thu Huong, Tran Thi Quynh, A method to design an efficient airfoil for small wind turbines in low wind speed conditions using XFLR5 and CFD simulations, Energies, 17 (2024).
- [10]. D. Van Thin, L. Q. Sang, C. D. Van, D. N. Huu, Modifying NACA6409 Airfoil Configuration to Improve Aerodynamic Performance in Low Wind Speeds, in Conference Proceedings - 2023 IEEE Asia Meeting on Environment and Electrical Engineering, EEE-AM 2023, (2023) 1-5.
- [11]. D. Van Thin, N. H. Duc, L. Q. Sang, Aerodynamic Analysis of NACA64A010 Airfoil Using XFLR5 and ANSYS Fluent, GMSARN International Journal, 18 (2024) 258–266, <http://gmsarnjournal.com/home/wp-content/uploads/2023/09/vol18no2-13.pdf>
- [12]. Airfoil plotter (s4110-il) (airfoiltools.com), <http://airfoiltools.com/airfoil/details?airfoil=s810-nr>.
- [13]. D. Marten, QBlade: A Modern Tool for the Aeroelastic Simulation of Wind Turbines vorgelegt von, PHD thesis, TU Berlin, (2020).
- [14]. M. Drela, XFOIL: an analysis and design system for low Reynolds number airfoils, Low reynolds number aerodynamics. Proc. Conf., NOTRE DAME, U.S.A., Berlin, Germany, Springer-Verlag, (54) 1989.
- [15]. Dinh Van Thin, Nguyen Huu Duc, Le Quang Sang, Aerodynamic analysis of naca 6409 airfoil in wind turbine by using panel method, TNU Journal of Science and Technology, 227 (2022) 227–235, <https://doi.org/10.34238/tnu-jst.5591>
- [16]. T. Chen, C. Wang, T. Liu, On physics of boundary vorticity creation in incompressible viscous flow, Acta Mechanica Sinica/Lixue Xuebao, 40 (2024) 323443.

- [17]. W. F. Merzkirch, Mach's Contribution to the Development of Gas Dynamics, in Ernst Mach: Physicist and Philosopher, Boston Studies in the Philosophy of Science, Springer, Dordrecht, 6 (1970) 42–59.
- [18]. M. Ahmad, Z. L. Hussain, S. I. A. Shah, T. A. Shams, Estimation of stability parameters for wide body aircraft using computational techniques, Applied Sciences, 11 (2021) 1-26.